

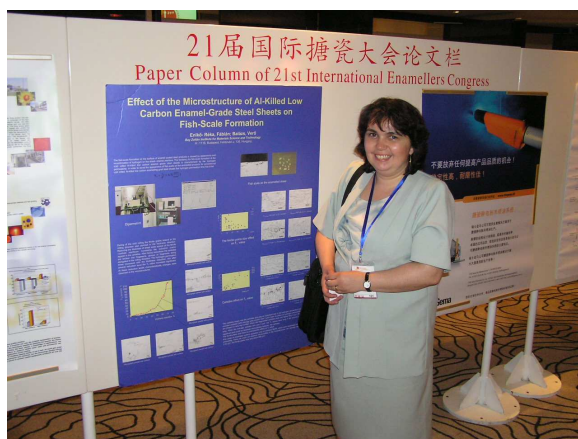
Effect of the Microstructure of Al-killed Low Carbon Enamel-Grade Steel Sheets on Fish-Scale Formation

Enikő Réka Fábián, PhD student

Budapest University of Technology and Economics, Budapest, Hungary

Balázs Verő

Bay Zoltán Foundation for Applied Research, Budapest,



XXI International Enamellers Congress

2008 Május 18-22, Shanghai, Kína



Effect of the Microstructure of Al-Killed Low Carbon Enamel-Grade Steel Sheets on Fish-Scale Formation

Enikő Réka, Fábrián¹; Balázs, Verő²

¹PhD student, Budapest University of Technology and Economics, Department of Material Science and Engineering; research fellow at Bay Zoltán Foundation for Applied Research, Institute for Materials Science and Technology; H -1116, Fehérvári u. 130, Budapest, Hungary; Tel: 00-36-1-4630557, Fax: 00-36-1-4630529, e-mail: enire@freemail.hu;

² MSc, Associate Professor at Bay Zoltán Foundation for Applied Research, Institute for Materials Science and Technology; H -1116, Fehérvári u. 130, Budapest Hungary, Tel: 00-36-1-4630559, Fax: 00-36-1-4630529, e-mail: vero@bzaka.hu

Keywords microstructure; hydrogen permeability, Al-killed low carbon steel

Abstract The tendency for fish-scale formation in case of the cold rolled Al-killed low carbon enamel grade steel sheets has been characterized by the hydrogen permeability. There are a good correlation between the microstructure and the hydrogen permeation time. The cold rolling effect on the microstructure and on the T_H value have been studied on samples prepared from Al-killed low carbon steel sheets with high coiling temperatures after several cold rolling levels. The microstructure of the hot rolled sheet was formed from ferrite and large carbides. The T_H value of the hot rolled strip was very short. Due to the cold rolling at the beginning of the process the dislocation densities increase. After some % of reducing in thickness at the ferrite –carbide interfaces appear voids. Increasing the reduction in thickness cracks appears in the carbides. After heavy reductions the carbides are broken into fragments, groups of fragments being elongated in the rolling direction. Increasing the reducing grade of the sheets' thickness the hydrogen permeation time calculated for 1 mm thickness increased. After some reduction level the T_H value increased significant. At these reduction levels in each case something has changed in the microstructure characteristics. Serve as an example at about 31% reduction $T_H = 4.04 \text{ min/mm}^2$; at 37% reduction $T_H = 11.56 \text{ min/mm}^2$. There we could observe broken carbides and microcavities between them. At 51% reduction for the microstructure has become characteristic the broken carbides, $T_H = 24.4 \text{ min/mm}^2$. Other jumping were observed at 60% reduction ($T_H = 47.9 \text{ min/mm}^2$) where the ferrite grains elongation became characteristic.

The ferrite grain size and the carbide morphology effect on T_H value were studied on low carbide enamel-grade steel sheets prepared in industrial conditions (in time of the cold rolling the thickness reduction of the coils were about 70%), after annealing (the steel sheets quality were DC01EK and DC04EK). The massive carbides with 4-7 μm^2 dimensions have serious effects on T_H values, but the small carbides have no effect on hydrogen permeability. The ferrite grains size has no significant effect on T_H value.

Objectives It is well known that the fish-scale formation on the surface of enamel coated steel products is caused by appearance and recombination of hydrogen at the sheet-enamel interface. The hydrogen can be absorbed in the metal during the enamel firing. The hydrogen is not homogeneously distributed in steel, as it would be in perfect iron crystal. In steel various trapping sites exist for hydrogen atoms. Hydrogen will be found not only in the normal interstitial lattice sites but also in atomic and micro-structural imperfections such as vacancies, solute atoms, dislocations, grain boundaries, boundaries of second phase particles, steel-inclusion interfaces and microcavities. The general term for this phenomenon is trapping. Trapping enhances the solubility of hydrogen but decreases the diffusivity. The tendency for fish-scale formation in case of the cold rolled Al-killed low carbon enamel grade steel



sheets is characterized by the hydrogen permeability. That is why hydrogen permeation test has been used for long time to estimate the hydrogen absorption capability of steel sheets used for enamelling. In order to avoid the appearance of fish-scale on the enamelled products for conventional cold rolled, Al-killed low carbon enamel-grade steel the hydrogen permeation time has to be $T_H = \frac{t_0}{d^2} \geq 6.7$ where „ t_0 ” is the hydrogen permeation time [min], “ d ” is the thickness of the steel sheet [mm].

Cold work increases the adsorption and absorption of hydrogen. The presence of dislocations is, to a large degree, responsible for the hydrogen diffusivity in iron at room temperature [1]. Kumnick and Johnson [2] studied high purity iron, deformed systematically in steps by cold rolling at room temperature. They employed a high purity iron deformed at room temperature to produce dislocations substructures with preponderance at edge dislocations as the major trapping sites. With increasing deformation, the dislocations form a dense cell structure. There were no other imperfections of sufficient density to trap significant amounts of hydrogen. The results for annealed and cold worked irons gave trap densities in the range 10^{20} - 10^{23} dislocations/ m^3 as a function of cold work, as expected for dislocations. The microstructure of steels differs from the high purity iron, so there are other trapping sites too for the hydrogen. At Al-killed low carbon enamel-grade steel sheets, in order to avoid the fish-scale on the enamelled products, the microstructure of the hot rolled strip should be formed from ferrite and carbides [3]. At these steels the microstructure is formed from ferrite and large carbides when the coiling temperature of the hot rolled sheet is high. To reach high T_H value for the sheets in industry is applied a thickness reduction about 70% [4]. But before were not studied the relationship between the microstructure and the hydrogen permeation time at these steels.

Materials and Testing Procedures

In our experiments we have studied the hydrogen permeability and the microstructure at different deformation levels (cold rolling) of Al-killed low carbon enamel-grade steel sheets. The steel were elaborated in LD steel converter, followed by continuous casting, hot rolling and pickling at Steelworks in DUNAFERR Ltd. The coiling temperatures were high (exceed 700°C), so we expected for the hot rolled strip the appearance of carbides at the ferrite grains boundaries [3, 5.]

The effect of the plastic deformation on the microstructures and the hydrogen permeability have been studied one steel sheet samples cold rolled on several rolling levels by duo rolling mill in Laboratory at Budapest University of Technology and Economics, Department of Material Science and Engineering. The chemical composition of the steel is given in Table 1.

Table 1 The chemical composition of the hot rolled sheet

Identification/ quality	Thickness of sheets [mm]	C	Mn	Si	S	P	Cu	Cr	Ni	Al	N	O	Fe
Hot rolled/ EK4	2.3	0.05	0.21	0.008	0.012	0.016	0.05	0.037	0.026	0.038	0.0042	0.0024	rest

To study the ferrite grain size and the carbide morphology effects on the hydrogen permeability of Al-killed, unalloyed low carbon steel sheets were examined samples from different parts of three cold rolled coils prepared for enamelling. The steel sheets qualities were DC01EK and DC04EK (EN 10209 - 96). The chemical composition of the coils is given in Table 2.

Table 2 The chemical composition of the annealed sheets

Identification/ quality	Thickness of sheets [mm]	Chemical composition [%]										
		C	Mn	Si	S	P	Cu	Cr	Ni	Al	N	Fe
A/ DC01EK	0.70	0.043	0.217	0.007	0.009	0.011	0.02	0.037	0.024	0.031	0.0062	rest
B/ DC01EK	0.80	0.044	0.196	0.007	0.011	0.015	0.05	0.038	0.048	0.039	0.0037	rest
C/ DC04EK	1.0	0.037	0.172	0.010	0.011	0.010	0.02	0.033	0.029	0.047	0.0054	rest

Each of the examined coils was elaborated in LD steel converter, followed by continuous casting, hot rolling and pickling at Dunaferri Steelworks Ltd. The coils were cold rolled at Dunaferri-Voest Alpine Ltd. For the cold rolled sheets the thicknesses reduction was about 70%. After cold rolling the examined coils were annealed in gutter-wound coil, in bell-type annealing furnace. The annealing temperature was 670°C; the holding time in each case was 16 hours. The annealing was succeeded by skin-pass rolling.

The optical microscopic examinations were carried out on longitudinal, transversal cross sections and parallel to the surface of the sheet using a LEICA MF-4 microscope.

The carbides morphologies were determined applying Quantimet 550 image analyser at the Innovation Management of Dunaferri Co.

The hydrogen permeation time was determined using electrochemical technique by DIPERMET-H hydrogen permeability measuring equipment (developed by Bay Zoltán Institute for Material Science and Technology) [6]. The samples were polished mechanical and washed in hot water and alcohol.

The fish scale formation tests were executed on degreased samples and on degreased and pickled samples at Lampart Budafoki Zománc Ltd.

Results

Plastic deformation effect

We have studied the effect of the cold rolling on the hydrogen permeation time calculated for united steel sheet thickness and on the microstructure. We studied the *microstructure* of the samples on longitudinal, transversal cross sections and parallel to the surface. The microstructures of the hot rolled strips were homogeneous, formed from ferrite, carbides, few pearlite and non-metallic inclusions. The carbides and pearlite were located at the equi-axial ferrite grains boundaries. The equi-axial *ferrite grain size* was $d_{gen}=26,6\mu m$. The hydrogen permeation times were very short ($T_H = 0.6$). Increasing the reduction of the thickness of the sheets the hydrogen transmission time increased, but at some reductions of the thickness appeared jumping in the T_H value (Fig 1). At 12% reduction in comparison with hot rolled strip the *microstructure* has not changed, but at few places it could be discovered cracks in the carbides (Fig. 2). At

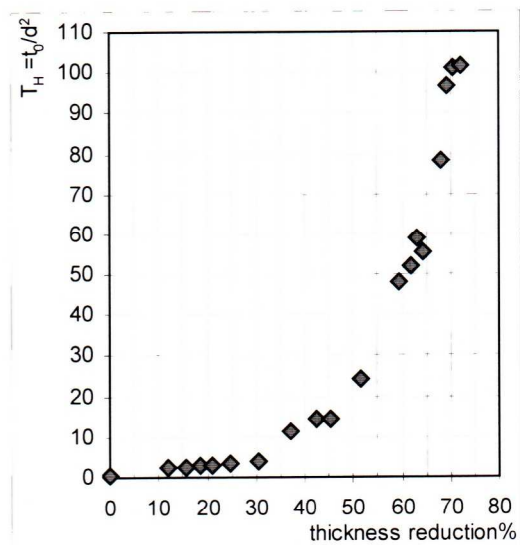


Fig.1 The cold rolling effect on the hydrogen permeation time

18%- 20% reduction of the thickness we could discern 1-2 broken carbides. After a reduction about 25% we could observe more but not too much broken carbides. The cracks appeared perpendicular on rolling direction and on the surface. Sometimes we observed microcavities in ferrite closed by the broken-points. Sometimes cracks in carbide are not observed by microscope, but voids appeared at the ferrite-carbide interface. The equi -axial ferrite grain size was $d_{gen}=26,6\mu m$. After 31% reduction of the thickness we observed a moderate ferrite grain elongation in longitudinal direction (Fig.3 a.). At 37% reduction appeared a sharp increasing in T_H value ($T_H =11.56$). There we could discern more broken carbides and between the carbide fragments microcavities have appeared.

Increasing the reduction of the thickness the ferrite grains extension in rolling direction became progressively more apparent (Fig. 3). The hydrogen permeation time increased significantly ($T_H =24.4$) after 51% thickness reduction. The broken carbides became characteristic after 51% thickness reducing. Microcavities appeared among the carbide fragments. At 60% reduction the hydrogen permeation time approximately had doubled ($T_H =47.9$). At these samples near the broken carbides the ferrite grain elongation became characteristic. At about 70% reductions the carbides were broken into fragments and the groups of fragments were elongated in the rolling direction. The ferrite grains elongation became more visible. For the last 3 reductions levels on the longitudinal samples has become visible shear bands. The calculated hydrogen permeation time was 101.

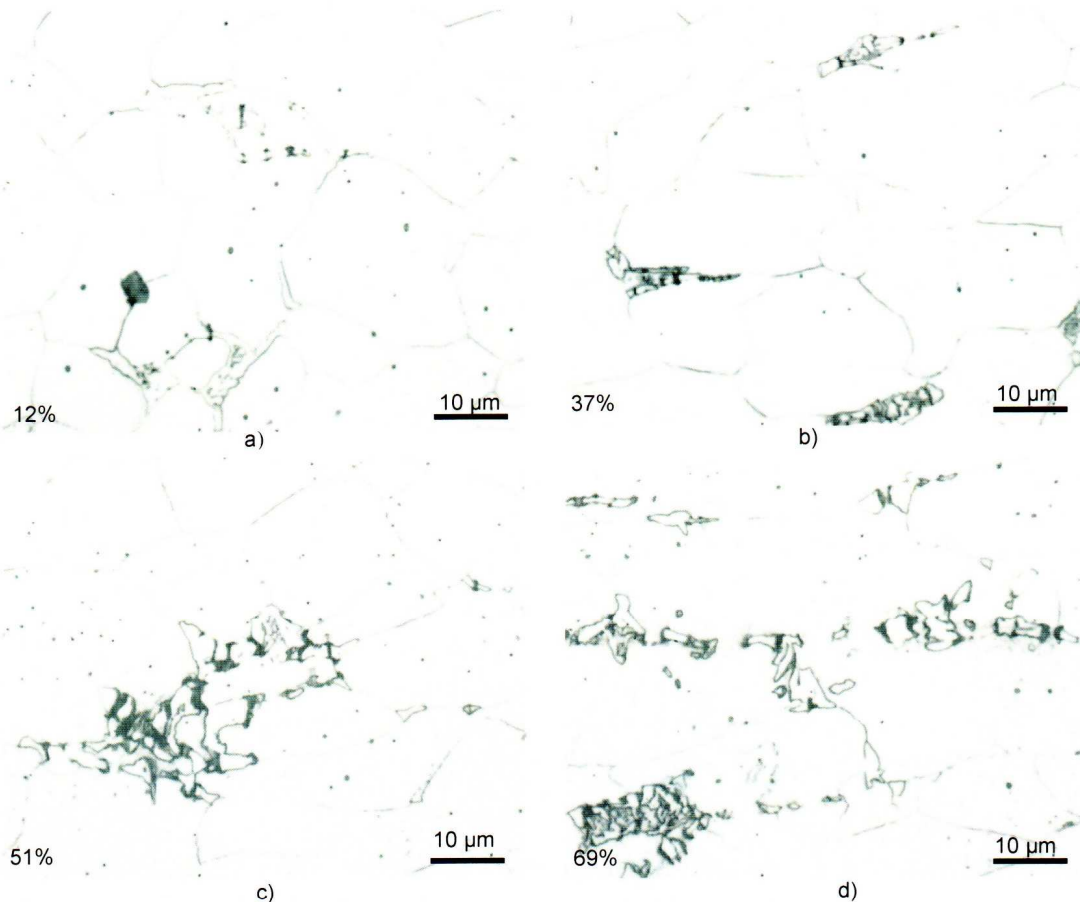


Fig. 2 Carbides morphologies after different thickness reduction. Micrographs parallel with the rolling surfaces
a)12% b)37% c)51% d)69%

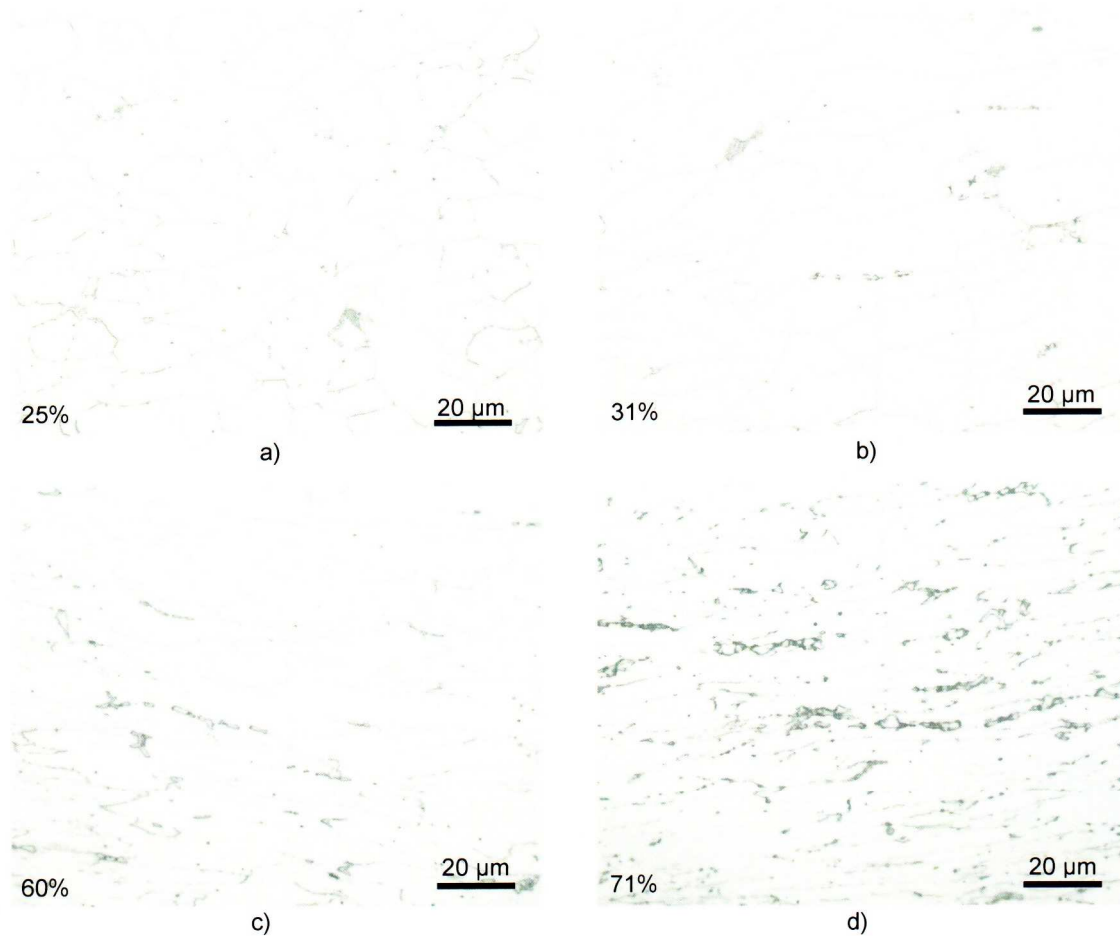


Fig. 3 Microstructures of samples in rolling direction after some characteristic reduction level
a)25% b)31% c)60% d)71%

Presence of microcavities plays important role to avoid the fish scale formation. If they are present in big amount they not disappeared during annealing and during enamel firing thermal cycle [7].

Effect of carbides and ferrite grain sizes were studied on Al-killed low carbon enamel grade steel sheets after annealing under industrial condition. The thicknesses reductions of the sheets during of the cold rolling were about 70%.

In order to study the microstructure the samples were prepared from the beginning (*samples notification: b*), from the middle (*samples notification: m*) and from the end of the coils (*samples notification: e*) 2.2 m long sheets before and after skin-pass rolling. The samples were taken from the middle transversal strips of the sheets, and they are nominated with *a* after annealing and with *s* after skin-pass rolling.

T_H values were measured prior to and after skin-pass rolling at the beginning, in the middles and at the end of the coils. We have measured the hydrogen permeability in each case in the middle (*samples notification: M*) and at the edges (*samples notification: E*) of the transversal bands of sheets (3 samples in each positions). The T_H values of the samples taken from the middle of cold rolled coils, and from the middle of the transversal strips were long; but generally the T_H values of samples taken from the end or from the beginning of the coils, were much lower.

The microstructures of the samples were formed from ferrite, carbides and non-metallic inclusions. The microstructures of the cold rolled sheets were not homogeneous. There were differences in the microstructure between the middle of sheets and at the edges of sheets, and middle of the coils and at beginnings and at the ends. The differences are likely to be caused by the technology. During hot rolling the temperature is different in the middle and at edges of coils. The microstructures at the beginning of the coils and at the end of the coils due to the manipulation, differ from the microstructure in the middle of the coils. Annealing in gutter-wound coil in bell-type furnace also influences the microstructure.

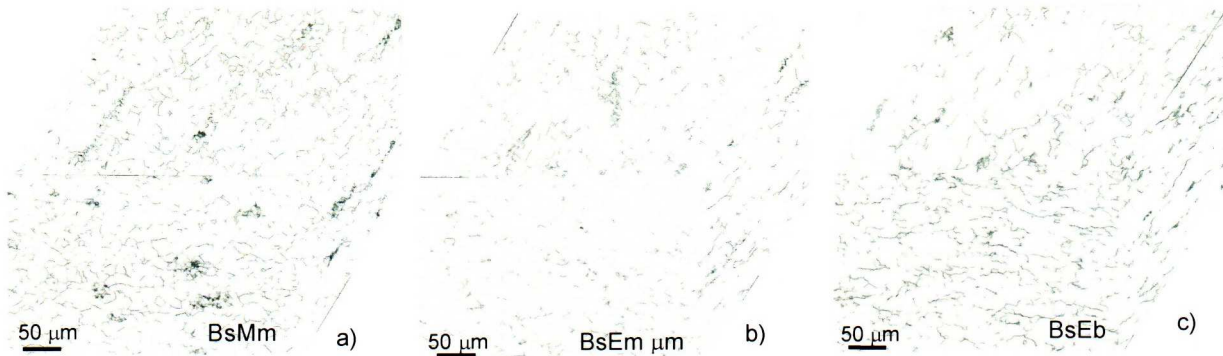


Fig 4. Microstructure of the coil with thickness 0.8 a) middle of the coil, middle of the strip
b) middle of the coil; edge of the strip c) beginning of the coil, edge of the strip

The ferrite grains' size of the samples are given in Table 3

Table 3 Ferrite grains' size after annealing at different part of the coils

	Samples state	Samples position in the rolls	A		B		C	
			T _H	Av. grain size [m ²]	T _H	Av. grain size [m ²]	T _H	Av. grain size [m ²]
Middle of the sheet	Annealed	Beginning	7.8	3900	8.6	735	9.9	367
		Middle	33.5	735	39.2	244	31.3	244
		End	4.3	1465	13.5	735	15.9	367
	Skin-pass rolled	Beginning	17	3900	7.5	980	18.6	980
		Middle	47.1	183	43.5	244	33.7	244
		End	17.7	735	21	1950	32.4	1465
Edge of the sheet	Annealed	Beginning	8.8	7810	13.4	735	11.8	980
		Middle	41.4	367	12.5	980	11.7	735
		End	18.5	735	8.6	1950	7.5	1465
	Skin-pass rolled	Beginning	12.9	5855	12.1	2925	7.8	2925
		Middle	55.9	735	11.2	980	10.5	735
		End	3.3	1465	7.1	1950	5.4	3900

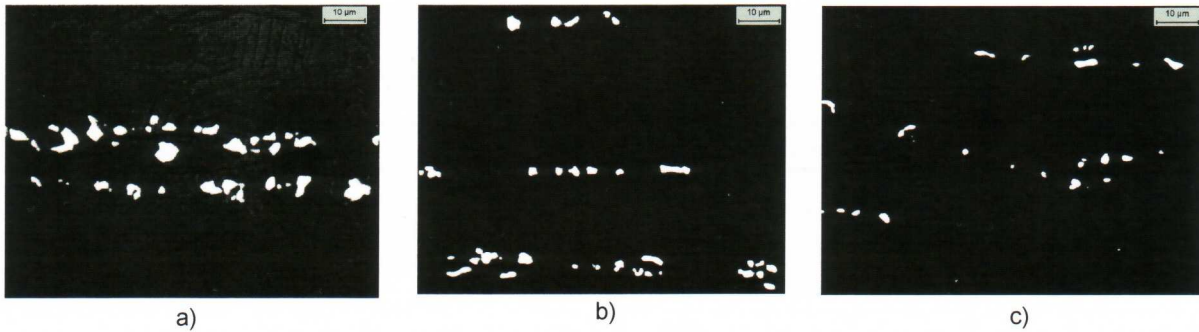


Fig. 7 Carbides morphology on longitudinal section; Klemm¹
a) AaMm; b) AaEm; c) AaEe;

The broken carbides areas typically were higher than $3 \mu\text{m}^2$ in the middle of the coils and in the middle of the sheets. In the middle of the coils and at the edge of the sheets the carbides groups were generally smaller than in the middle of the sheets. The carbides areas of the sheets with 1 mm thickness (C) were between $2\text{-}3 \mu\text{m}^2$, while for sheets with 0.8 mm thickness (B) were between $1\text{-}2 \mu\text{m}^2$ and for the sheets with 0.7 mm thickness (A) were between $4\text{-}7 \mu\text{m}^2$.

Characteristics of samples regarding the carbides are given in table 4

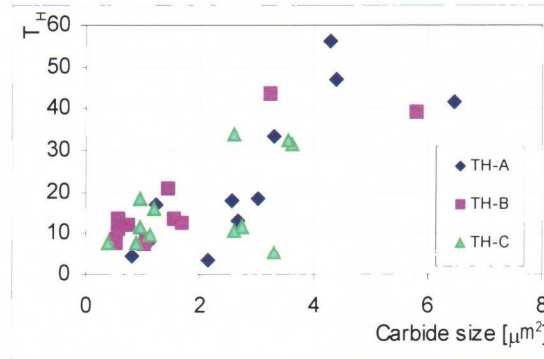


Fig. 8 The carbide size effect on T_H values

Table 4 Characteristics of samples regarding the carbides and T_H values

Samples mark	T_H	Carbides							
		Longitudinal sections				Transversal sections			
		Average area [m^2]	Average perimeter [m]	Number/ mm^2	Carbide perimeter/unit area [mm/mm^2]	Average area [m^2]	Average perimeter [m]	Number/ mm^2	Carbide perimeter/unit area [mm/mm^2]
AaMb	7.8	1.09	4.59	27623	113.7	1.11	4.30	12838	55.2
AaMm	33.5	3.03	7.22	6384	46.2	3.53	8.32	2616	21.8
AaMe	4.3	0.79	3.77	3584	13.8	0.90	3.64	12868	46.8
AsMb	17	1.23	4.51	12440	52.1	1.60	5.28	5080	26.8
AsMm	47.1	4.37	9.08	2405	21.8	4.97	9.84	2568	25.3



continue

Samples mark	T _H	Carbides							
		Longitudinal sections				Transversal sections			
		Average area [m ²]	Average perimeter [m]	Number/mm ²	Carbide perimeter/unit area [mm/mm ²]	Average area [m ²]	Average perimeter [m]	Number/mm ²	Carbide perimeter/unit area [mm/mm ²]
AsMe	17.7	2.56	6.90	2785	19.0	3.36	7.78	2738	21.3
AaEb	8.8	1.07	4.52	6082	26.7	1.36	5.12	7983	40.8
AaEm	41.4	6.46	11.65	2308	27.3	4.36	9.21	1771	16.3
AaEe	18.5	3	6.96	4442	31.0	2.56	6.59	6072	40
AsEb	12.9	2.68	6.65	4928	31.8	2.87	7.06	5646	39.9
AsEm	55.9	4.28	8.41	3695	30.5	2.82	5.84	7234	42.2
AsEe	3.3	2.15	5.67	7171	40.8	1.53	5.08	7575	38.5
BaMb	8.6	0.52	3.06	10355	31.9	0.66	3.30	10191	33.7
BaMm	39.2	5.79	9.93	1700	16.8	44.6	8.94	2136	19.1
BaMe	13.5	1.55	5.19	5155	26.8	0.86	4.01	3784	15.2
BsMb	7.5	0.54	3.14	7386	23.4	0.45	2.88	8244	23.8
BsMm	43.5	3.24	8.06	1852	14.8	3.78	8.88	1156	10.3
BsMe	21	1.43	5.00	4291	21.5	1.16	4.55	3249	14.8
BaEb	13.4	0.57	3.20	10215	32.9	0.52	3.01	9339	28.2
BaEm	12.5	1.7	5.24	5520	25.5	1.46	5.09	2537	12.9
BaEe	8.6	1.06	4.06	8366	33.2	1.00	3.96	8025	31.8
BsEb	12.1	0.72	3.58	10548	37.9	0.53	3.23	7289	23.5
BsEm	11.2	0.56	3.12	8944	27.6	0.37	2.64	11189	29.6
BsEe	7.1	1.02	3.96	9556	37.6	0.84	3.85	8798	33.9
CaMb	9.9	1.14	4.92	2405	11.9	0.95	4.65	2701	12.5
CaMm	31.3	3.62	9.63	1700	16.3	2.75	10.17	13.14	13.4
CaMe	15.9	1.2	5.01	1438	6.6	0.38	3.19	2799	8.9
CsMb	18.6	0.96	4.78	3344	16.0	0.86	4.66	2561	11.9
CsMm	33.7	2.58	6.80	1489	9.9	2.59	7.00	1412	9.9
CsMe	32.4	3.53	9.03	1685	15.2	3.30	9.12	1308	11.9
CaEb	11.8	0.95	3.82	2701	27.0	0.47	2.80	10830	30.3
CaEm	11.7	0.80	3.54	1314	20.5	0.76	3.56	6176	22.0
CaEe	7.5	1.36	4.65	2799	10.2	1.44	4.62	2525	11.7
CsEb	7.8	0.81	3.71	2561	25.4	0.66	3.38	6419	21.7
CsEm	10.5	1.05	4.06	1412	22.0	0.76	3.67	5896	21.7
CsEe	5.4	1.19	4.16	1308	19.8	0.82	3.55	4971	17.6

At the samples where big massive carbides could be observed (average areas higher than $4 \mu\text{m}^2$), the hydrogen permeation times were long. The small, rounded carbides (with average area smaller than $1 \mu\text{m}^2$) have no effect on hydrogen permeability even if they are present in very big number (see samples: AaMb and AaEb). When the average carbide size was about $3 \mu\text{m}^2$ the T_H values depend on the number and morphology of the carbides, and/or if there were microcavities in the microstructure. When the carbides sizes were on average $3 \mu\text{m}^2$ and the amount of carbides were significant the T_H value were high. In case of reduced number of carbides T_H values were smaller. Moreover microcavities between the carbides could be observed by optical microscope if the hydrogen permeation time was long.

The ferrite grains size has no characteristic effect on T_H value. Although where the T_H values were high, the ferrite grains size were fine, in each case there were massive carbides groups, and between the carbide fragments microcavities. Where the ferrite structures were coarse-grained, in the microstructure we could observe a big amount of small carbides, which did not form groups, the hydrogen permeation time was short.

Fish scale on enamelled surface appeared only on samples BsMb, which were degreased and pickled prior to enamelling. There, the average carbides size was $0.54 \mu\text{m}^2$, the ferrite grains size was about $980 \mu\text{m}^2$ and microcavity could not be observed.

Conclusions

The technological operations have complex effect on the different type of traps, which coexist in the enamel grade steels. Therefore the effects of carbides, micro-cavities, grain boundaries and dislocations cannot be separately discussed.

During the cold rolling the dislocation density increases. After heavy reductions of thickness, films of cementite located at the ferrite grains boundaries tend to be broken into fragments. With appearances of microcavities among the fragmented carbides the hydrogen permeation time increased significantly (after 51% reduction $T_H = 24.4 \text{ min/mm}^2$). For the samples where the broken carbides and microcavities among the carbides fragments became characteristic the hydrogen permeation time increased again significantly. At this reduction level (60%) T_H was about 48 min/mm^2 . After about 70% reduction of thickness the T_H value presented again a significant increase ($T_H = 101 \text{ min/mm}^2$). There the ferrite grain elongation became more visible.

The carbides shape and the carbides size play an important role in the hydrogen permeation time. The small, rounded carbides (with average area smaller than $1 \mu\text{m}^2$) have no effect on hydrogen permeability even if they are present in very big number. When the fragmented carbides sizes are higher than $4 \mu\text{m}^2$ the T_H values are long.

The ferrite grains size has no characteristic effect on T_H value.

Acknowledgement

A part of these studies take parts from the "Enamel Grad Steels, Technology and Examination Methods" research and development work, which is cordoned by Innovation Management at Dunafer Ltd. and supported by ME (Ministry of Education).

References

- [1] Z. Szklarska-Smialowska and Z. Xia: *Corrosion Science*, Vol. 39, 1997, p 2171
- [2] A. J. Kurnick and H. H. Johnson: *Acta Met.* Vol 28, 1980 p33
- [3] Verő Balázs: D Sc Thesis, Budapest, 1994, p 53-54



- [4] Hazai alapanyagból egy rétegben zománcozott melegvíztároló gyártástechnológiájának kidolgozása VASKÚT, 1984, T.SZ.11-05-1844
- [5] Leonard E. Samuels: Light Microscopy of Carbon Steels, ASM International; Materials Park OH44073-0002, 1999 p. 44-46
- [6] A Fauszt, B. Verő, R. Takács, Á. Horváth, H. Schneider: Effect of the Enamel Firing Thermal Cycle on the Microstructure and the Hydrogen Permeability of Enamel-Grade Steels; 2002 Trans Tech Publications Ltd; p 165-170
- [7] E-R Fábrián, A Fauszt, B. Verő, L. Dévényi, H. Schneider: Effect of a Firing Thermal Cycle on the Microstructure and on the Hydrogen Permeability of 1.0392 Enamel-Grade Steel Sheets, Proceedings of the IVth Conference on Mechanical Engineering;. Gépészet 2004, p. 57-62